de Saint-Jean et al., http://www.jcb.org/cgi/content/full/jcb.201104062/DC1

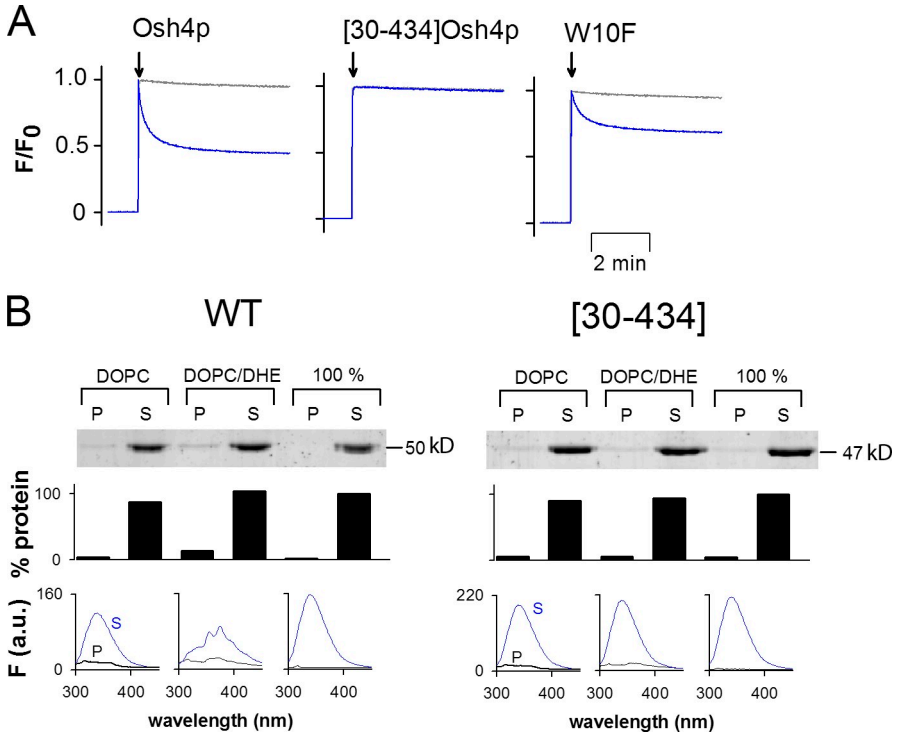

Figure S1. **The lidless [30–434]Osh4p mutant is unable to extract DHE.** (A) Normalized fluorescence at 340 nm of 0.5 µM Osh4p, [30–434]Osh4p, or Osh4p(W10F) once added to large DOPC/DHE (99.5:0.5 mol/mol) liposomes (0.5 mM lipids total lipids, blue trace) or to DOPC liposomes (black trace). The contribution of liposomes or buffer to the fluorescence signal was subtracted from each curve. The fluorescence of each trace was normalized by considering the fluorescence of Osh4p in buffer at time 0 as the maximal intensity. The lack of quenching of [30–434]Osh4p by DHE could indicate that Trp10, one of the residues of the lid in contact with sterol, was the sole tryptophane whose emission was quenched by DHE. However, a drop of signal was seen with Osh4p(W10F), which demonstrates that the lack of quenching of [30–434]Osh4p was caused by its inability to stably sequester sterol. (B) Solubilization of DHE by Osh4p or [30–434]Osh4p (0.5 µM) from DOPC liposomes containing 0.5% DHE using the same protocol as in Fig. 1 E. Compared with wild-type Osh4p, the spectrum of [30–434]Osh4p was identical to the spectra recorded after incubation with DHE-free liposomes or in the absence of liposomes. This indicated that [30–434]Osh4p did not solubilize DHE. The data shown are from a single representative experiment out of two independent experiments. P, pellet; S, supernatant.

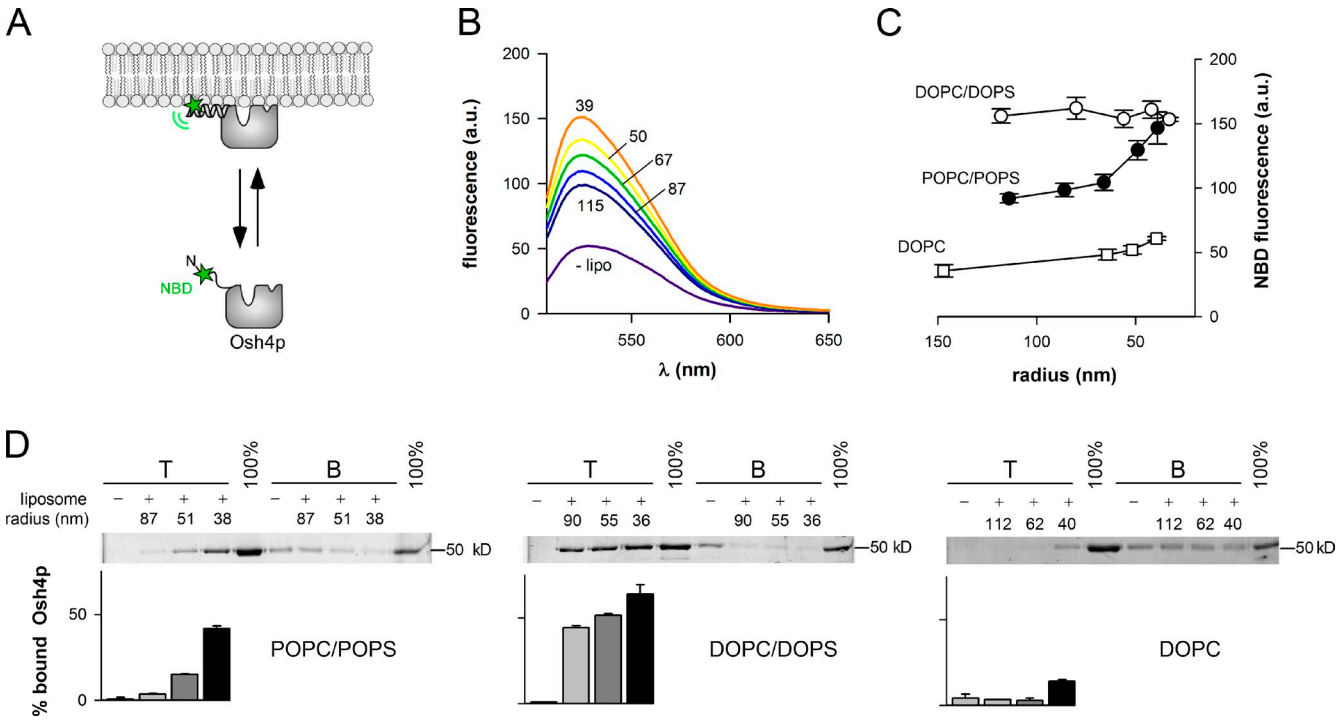

Figure S2. **A fluorescence-based approach to measure the avidity of Osh4p for lipid membranes.** (A) To follow membrane binding, we replaced the endogenous solvent-exposed cysteine 98 of Osh4p with a serine and introduced a cysteine in place of an alanine at position 5 within the lid. This cysteine was labeled with NBD, a probe highly sensitive to the environment polarity. (B) We measured upon excitation at 495 nm the fluorescence spectrum of NBD-Osh4p (0.5 µM) with or without POPC/POPS liposomes (70:30 mol/mol; 500 µM) of defined radius. In the presence of large liposomes (R_H = 115 nm), the signal was approximately twofold higher than without liposome and reached a much higher value with smaller liposomes (up to fourfold with R_H = 39 nm). (C) NBD intensity measured at 525 nm is reported as a function of liposome radius and for different membrane compositions. With liposomes containing the same amount of negatively charged lipids but of lower lipid-packing (DOPC/DOPS 70:30 mol/mol), we observed maximal binding whatever the liposome radius. With neutral liposomes (DOPC), binding was low but still dependent on curvature. Data are represented as mean ± SEM (error bars; *n* = 2). (D) Flotation assays. 0.75 µM Osh4p was incubated with liposomes (0.75 mM lipids) similar to what was used in B and C. After centrifugation, the liposomes were recovered by centrifugation at the top of a sucrose cushion and analyzed by SDS-PAGE. The error bars show the variation observed between two independent experiments. In agreement with the NBD fluorescence assay, Osh4p bound preferentially to negatively charged membranes with a high positive curvature and/or low lipid packing. This indicated that the NBD probe was well-positioned within Osh4p to monitor membrane binding.

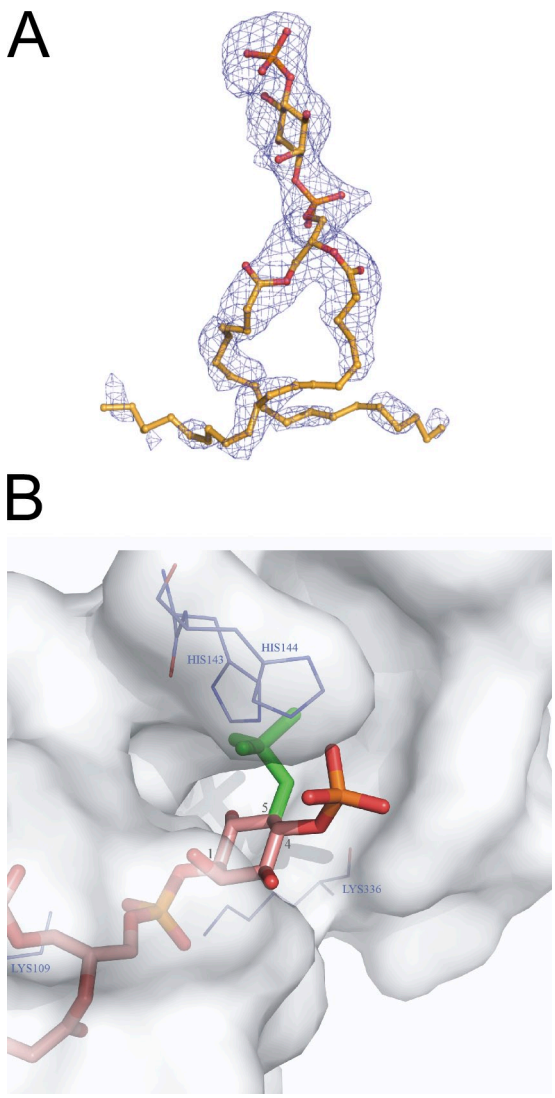

Figure S3. **Additional data on the interaction between PI(4)P and Osh4p.** (A) Differential interaction of PI(4)P with Osh4p. Although the polar head of PI(4)P is engaged in many specific interactions with several Osh4p residues, the aliphatic side chains interact loosely with the protein. The blue electron density represents an Fo-Fc omit map contoured at 1.5 σ. The omit map was generated by using the PHENIX simulated annealing protocol with the PI(4)P ligand being omitted. Oxygen, carbon, and phosphorus atoms are shown in red, yellow, and orange, respectively. (B) Specificity of Osh4p for PI(4)P versus PI(4,5)P_2. Modeling of the position of the 5-phosphate group of the PI(4,5)P_2 (green) superimposed to the crystallographic mode of binding of PI(4)P (red and orange) in the structure of the Osh4p–PI(4)P complex. The surface of Osh4p is displayed in white. Residues found to recognize PI(4)P are shown in purple.

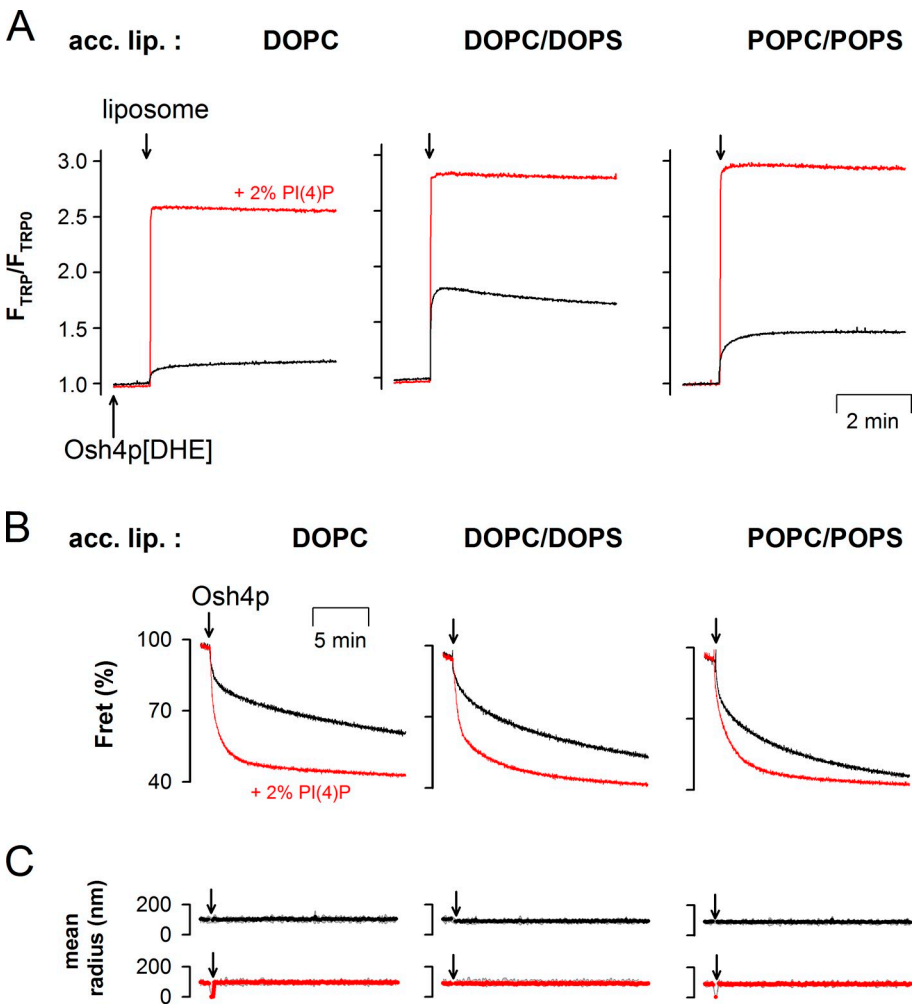

Figure S4. **Influence of the acceptor liposome composition on the ability of Osh4p to release DHE into acceptor membranes, transport DHE, and bridge liposomes.** (A) DHE release assay. The experiments were performed as in Fig. 5 A. Large liposomes (240 µM) were added to Osh4p preloaded with DHE (~0.5 µM) at 30°C. The liposomes contained DOPC, DOPC/DOPS (70:30), or POPC/POPS (70:30), and were supplemented with (red traces) or without (black traces) 2% PI(4)P. (B) Transport assays were performed as in Fig. 6 but with a lower liposome concentration to minimize light scattering, thereby allowing a dynamic light scattering (DLS) experiment. Large DOPC/DNS-PE/DHE liposomes (87.5:2.5:10 mol/mol, 10 µM lipids) were mixed with large liposomes (225 µM lipids) of defined composition and with (red trace) or without 2% PI(4)P (black trace). After 3 min, 0.5 µM Osh4p was added. The accessible lipid-to-protein ratio was lower than in Fig. 6 C (250 instead of 1,000) and the amount of Osh4p per DHE molecule was higher, which explains why transport kinetics were faster. Note, however, that the composition of the acceptor membranes influenced DHE transport in a similar way as shown in Fig. 6 C (C). Each transport reaction shown in B was repeated and liposome aggregation was assessed by dynamic light scattering (DLS). The mean radius is represented over time. Osh4p transports sterol to PI(4)P-containing membranes without inducing any noticeable liposome aggregation.

Table S1. **Data collection and refinement statistics**

Criteria	Osh4p + PI(4)P
Data collection	
Space group	$P2_1$
Cell dimensions	
a, *b*, *c* (Å)	73.46, 54.76, 121.86
α, β, γ (°)	90.00, 91.00, 90.00
Resolution (Å)	47.29–2.60 (2.75–2.60)[a]
R_{sym}	0.146 (0.490)
$I/\sigma I$	6.8 (2.8)
Completeness (%)	99.8 (99.9)
Redundancy	3.7 (3.7)
Refinement	
Resolution (Å)	47.29–2.60 (2.75–2.60)[a]
No. of reflections	30,180 (4,633)
R_{work}/R_{free}	0.228/0.269
No. atoms	
Protein	6,077
Ligand	93
Water	241
B-factors	
Protein	39.3
Ligand	49.3
Water	32.1
Rms deviations	
Bond lengths (Å)	0.002
Bond angles (°)	0.596

Values in parentheses are for highest-resolution shell.